Springer

Journal of Mechanical Science and Technology 23 (2009) 3191~3198

Journal of Mechanical Science and Technology

www.springerlink.com/content/1738-494x
DOI 10.1007/s12206-009-1003-2

Assessment of the sulfide corrosion fatigue strength for a multi-pass welded A106 Gr B steel pipe below the low SSCC limit †

Gyu Young Lee[1] and Dong Ho Bae[2,*]

[1]*Graduate school, Mechanical engineering, SungkyunKwan University, 300 Chunchun dong,Jangan-gu, Suwon, Kyunggi-do 440-746, Korea*

[2]*School of Mechanical engineering, Sungkyunkwan Univertity, 300, Chunchun-dong, Jangan-fu, Suwon, Kyunggi-do, 440-746, Korea*

(Manuscript Received March 17, 2009; Revised September 1, 2009; Accepted September 11, 2009)

Abstract

In the area of heavy construction, welding processes are vital in the production and maintenance of pipelines and power plants. Welding processes happen to produce residual stresses and change the metal structure as a result of the large nonlinear thermal loading that is created by a moving heat source. The fusion welding process generates formidable welding residual stresses and metallurgical change, which increase the crack driving force and reduce the resistance to the brittle fracture as well as the environmental fracture. This is a serious problem with many alloys as well as the A106 Gr B steel pipe. This pipe that is used in petrochemical and heavy chemical plants either degrades due to corrosive environments, e.g., chlorides and sulfides, and/or become damaged during service due to the various corrosion damage mechanisms. Thus, in this study, after numerically and experimentally analyzing the welding residual stress of a multi-pass welded A106 Gr B steel pipe, the sulfide stress corrosion cracking (SSCC) characteristics were assessed in a 3.5 wt.% NaCl solution that was saturated with H_2S gas at room temperature on the basis of NACE TM 0177-90. The specimens used are of two kinds: un-notched and notched. Then, the sulfide corrosion fatigue (SCF) strength for the un-notched specimen was assessed below the low SSCC limit that was previously obtained from the SSCC tests for the notched specimen. From the results, in terms of the SSCC and SCF, all the specimens failed at the heat-affected zone, where a high welding residual stress is distributed. It was found that the low SSCC limit of un-notched specimens ($\sigma_{SSCCun\text{-}notched}$) was 46% (230 MPa) of the ultimate tensile strength (σ_U=502 MPa) of a multi-pass welded A106 Gr B steel pipe, and the notched specimens ($\sigma_{SSCCnotched}$) had 40% (200 MPa) of the ultimate tensile strength. Thus, it was determined that $\sigma_{SSCCun\text{-}notched}$ was 13% lower than $\sigma_{SSCCnotched}$. Further, the sulfide corrosion fatigue limit ($\sigma_{SCFun\text{-}notched}$) was 32% (160 MPa) of the ultimate tensile strength of welded specimens. This $\sigma_{SCF\ un\text{-}notched}$ was 20% lower than $\sigma_{SSCCnotched}$.

Keywords: Weld metal; Heat affected zone; Welding residual stress; Brittle fracture; Hydrogen sulfide; Smooth specimen; Sulfide stress corrosion cracking(SSCC); Sulfide corrosion fatigue(SCF)

1. Introduction

Welding is practically used in every industry and is associated with a very large part of the country's gross national product. In the area of heavy construction, welding processes are vital in the production and maintenance of pipelines and power plants. Welding processes happen to produce residual stresses and change the metal structure as a result of the large nonlinear thermal loading that is created by a moving heat source.

The fusion welding process generates formidable welding residual stresses and metallurgical change, which increases the crack driving force and reduces

† This paper was recommended for publication in revised form by Associate Editor Youngseog Lee

*Corresponding author. Tel.: +82 31 290 7443, Fax.: +82 31 290 7939
E-mail address: bae@yurim.skku.ac.kr

the resistance of the brittle fracture as well as the environmental fracture [1-3]. In particular, the welds are more sensitive than base metal to corrosive environments. This is a serious problem with many alloys as well as the A106 Gr B steel pipe. This pipe is used in petrochemical plants and is degraded by corrosive environments, e.g., chlorides, sulfides, and pH in crude oil, and/or damaged during service by various corrosion mechanisms. The pipe is particularly noteworthy in the area of crude-oil transportation. Therefore, an investigation of the pipe's fracture mechanism through corrosion fatigue or stress corrosion cracking and an evaluation of the fracture characteristics of the welds of the material are very important for: the diagnoses of safety and integrity of facilities; lifetime predictions of degraded materials, and the establishment of an economical period for inspection. As it happens, an evaluation of the environmental strength or analysis of the fracture mechanism of welds is difficult due to the complex residual stress distribution and metallurgical changes in welding processes. Moreover, the complicated test procedures and long test periods also become major reasons. One common problem associated with welding is welding residual stress as well as the distortion of finished products. At present, even though the data and information on environmental strength and fracture characteristics are needed for the safe design and damage protection of welded structures and facilities, they are poor in comparison with the others for the above reasons.

Thus, in this study, a sulfide stress corrosion cracking (SSCC) test, which is based on NACE TM 0177-90 [4], of a multi-pass welded A106 Gr B steel pipe was conducted in a 5.0 wt.% NaCl solution that was saturated with H_2S gas at room temperature. The SSCC characteristics were assessed.

2. Welding residual stress of the A106 Gr B steel pipe weld

2.1 The Finite Element Analysis (FEA) model

An eleven-pass welded A106 steel pipe model was considered in this study. The chemical composition and mechanical properties at room temperature are illustrated in Tables 1 and 2, respectively. This material is widely using in industrial facilities such as nuclear power plants and heavy chemical plants. The groove for welding was machined in a V-type. The welding conditions are given in Table 3. The temperature-dependent material properties of A106 Gr B steel pipe are shown in Fig. 2. The thickness was 17.5 mm and the inner diameter of the model was 272 mm. The first and second passes were welded by gas tungsten arc welding (GTAW) and the other nine passes (#3~#11) were welded by shielded metal arc welding (SMAW). Three-dimensional finite element analysis (FEA) models were used for analyzing the welding residual stress. The cross-section and the multi-pass welded pipe for the finite element model are shown in Fig. 1(a) and 1(b), respectively. The area with oblique lines represents the layers of the weld bead that are determined by the actual weld coupon. Finer meshes

Table 1. Chemical composition (wt. %) of the A106 Gr B steel weld.

C	Mn	Si	P	S	Ni	Cr	Mo	Cu
0.2	1.02	0.25	0.017	0.005	0.02	0.06	0.01	0.01

Table 2. Mechanical properties of the A106 Gr B steel weld and base metal.

	Yield strength (MPa)	Tensile strength (MPa)
Base metal	430	486
Weld	380	502

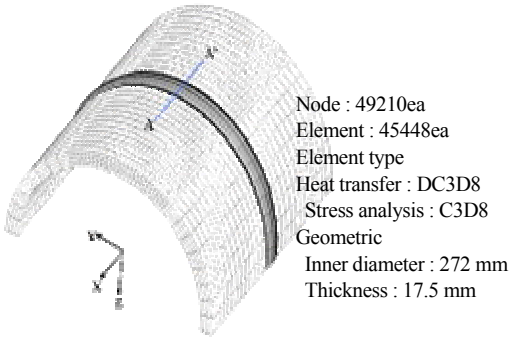

(a) Three-dimensional nonlinear FEA model

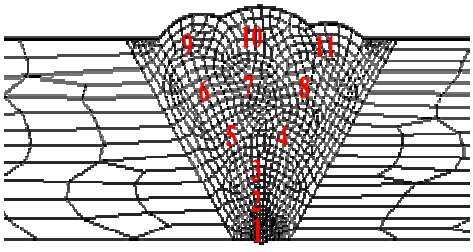

(b) Mesh generation of the weld.

Fig. 1. Three-dimensional nonlinear FEA model used for thermal history and welding residual stress analysis of a multi-pass welded joint.

Table 3. Conditions of multi-pass welding.

Pass no.	Amp. (A)	Volt (V)	Welding length (mm)	Time (min.)	Speed (cm/min)	Heat Input (KJ/mm)
1~2 GTAW	116 ~118	14 ~24	306	4.42	8.3~9.0	1.1~1.4
3~11 SMAW	125 ~135	24 ~26	306	2.39 ~4.55	7.2~11.5	1.6~2.2

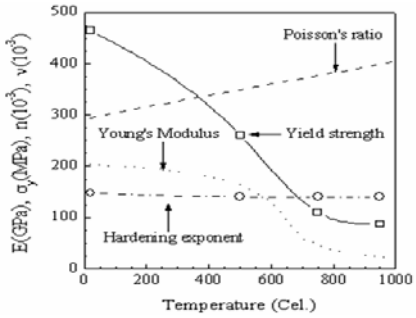

Fig. 2. Temperature dependent material properties.

that used eight-node elements were generated in the weld metal regions to handle the greater non-linearity and to obtain accurate results. I-DEAS® and Hypermesh®, which are commercial pre- and post-processors, respectively, were used for mesh generation. ABAQUS was employed for the transient-temperature analysis and subsequent residual stress analyses. The total number of elements was 45448 and the total number of nodes was 49210.

2.2 Assumptions and simulation procedures

Uncoupled thermal-mechanical analysis was conducted, which means that the temperature fields and histories were calculated from the thermal analysis and then used as input data for the subsequent stress analysis. Identical time-steps were used for both thermal and mechanical analyses. The numerical procedures for the uncoupled thermal-mechanical analysis are shown in Fig. 3. During the temperature analysis, it was assumed that the initial temperatures of base and weld metals were a constant room temperature (21°C). The temperature-dependent material properties were used in the analysis. However, the conductivity and specific heat in the molten pool were assumed to be constant. The effect of the latent heat of fusion, which is the internal energy change during melting or solidification, was also considered in the thermal analysis. The heat loss coefficient that was applied to all exposed surfaces was 0.0817 W/m²-°C

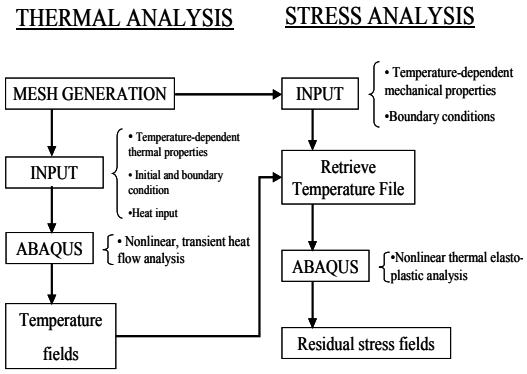

Fig. 3. The numerical procedures for the uncoupled thermal-mechanical analysis.

(0.0001 Btu/in²-°F). Other thermal boundary conditions, such as radiation and forced convection due to the shielding gas flow, were neglected. These terms only become significant when the behavior of the flow of a molten pool is of interest. Owing to the high temperatures in the molten pool, the behavior of the flow can be ignored in the residual stress simulations. Similarly, radiation and convection influences on the microstructures and cooling rates in the weld metal, as well as heat losses or gains from phase transformation, were neglected. The effect of radiation was incorporated in the thermal efficiency (η) and the volume change effect due to phase transformation was also neglected in the stress analysis. In the stress analysis, the mechanical and physical properties, viz., the yield stress, elastic and plastic moduli, and thermal expansion coefficient, were considered to be temperature dependent. Mechanical properties were, however, assumed to be constant above the melting point. The temperature dependency of Poisson's ratio was neglected. A constant value of 0.32 was used for A106 Gr B steel in the analysis. The element rebirth technique [5] was employed to include the multi-pass weld metal deposition effects. With this technique, the elements that simulated each weld pass were grouped at the model generation stage. During analysis, these element groups, which represented weld passes, were first removed and then reactivated at a specified moment to simulate a given deposition sequence of weld passes. When a group of weld elements was activated, specific initial temperatures were imposed at all nodes that were associated with the weld elements. The heat input fractions of the heat flux were empirically determined as ff =0.6 and fr = 1.4 [5].

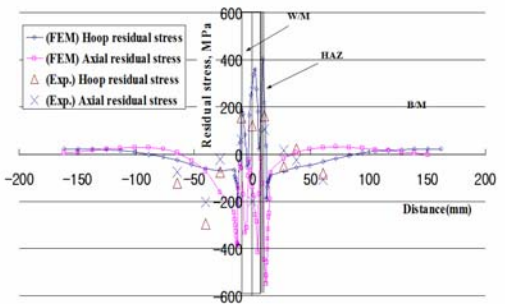

Fig. 4. Welding residual stress distribution in the multi-pass weld of A106 Gr B steel pipe.

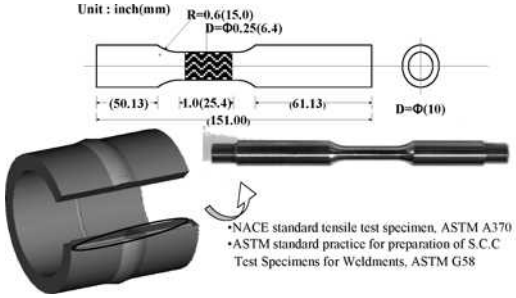

Fig. 5. Location of cutting in the specimen from the welded pipe and the configuration of the SSCC test specimen.

2.3 Results and discussion

The predicted radial and axial welding residual stress distributions on the top surface and the experimental results are compared in Fig. 4. The radial peak stress values as per FEA were around 402 MPa; however, the experimental result yielded 160 MPa. The axial peak stress value predicted by FEA was 80 MPa. Even though the peak stresses from FEA were, quantitatively speaking, substantially different from those yielded by the experiment, the trends in the predicted residual stress distributions were very similar to the experimental distributions. In multi-pass welding, the contraction of subsequent passes is always constrained by preceding passes. The residual stresses that are generated from the earlier passes dominate the residual stresses of the final pass. In this manner, since welding residual stress distributions in multi-pass welds are very complex and large, it is necessary to consider welding residual stress for the safe SSCC assessment of a multi-pass welded A106 Gr B steel in the weld design and damage analysis of a multi-pass welded A106 steel pipe.

3. SSCC assessment of a multi-pass welded A106 Gr B steel weld

3.1 Material and specimen

Fig. 5 shows the location of cutting in the specimen from the welded pipe and the configuration of the SSCC test specimen. The smooth specimen of Fig. 5 includes the weld metal, heat affected zone (HAZ), and the base metal within its gauge length. The welding procedures are GTAW+SMAW. The welding conditions are illustrated in Table 3. As shown in Fig. 5, all specimens were prepared in a perpendicular direction to the weld line. Since the asperity and oily particles on the pipe surface affect the corrosion reaction of metal, after the surface was polished, each specimen was cleaned up by an ultrasonic washer in acetone.

3.2 Test equipment

Stress corrosion cracking is defined as a mechanism of material damage that is due to a combination of the static stress and the corrosion environment. Therefore, the corrosion environment that is established under the static loading condition has to be constantly maintained during the whole test period. In the case of the SSCC test that uses the hydrogen sulfide (H_2S) gas, since hydrogen sulfide is very poisonous, it must not leak from the components such as the corrosion cell, tubes, and fittings, during the test period. The corrosion cell that was used in the SSCC test is as shown in Fig. 6. To maintain constant conditions for the SSCC test and to prevent degradation by corrosion, the corrosion cell was made from acryl and engineering plastic. The loading unit was made up with a ring-type frame, load cell, and indicator, following the recommendations of NACE TM 0177-90. In particular, by using flat-type springs that yield high stiffness for the loading units instead of bolts, the variation of the load that was applied to the test specimen could be constantly compensated for during the test period. Fig. 7 illustrates a schematic diagram of the SSCC test equipment, and Fig. 8 shows a general view of the equipment. Teflon tubes and fittings were used for the test equipment, and the connections between the tubes and corrosion cells were made with SUS316. One of the most important units in the SSCC test equipment is the neutralization unit. To maintain the chemical equilibrium of the test solution in the corrosion cells throughout the SSCC test period,

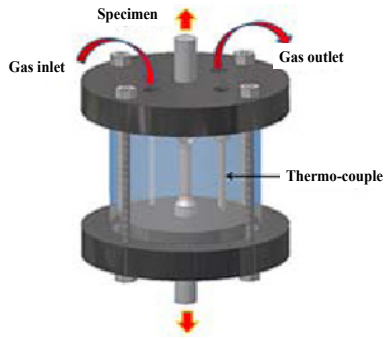

Fig. 6. Corrosion cell used in the SSCC test.

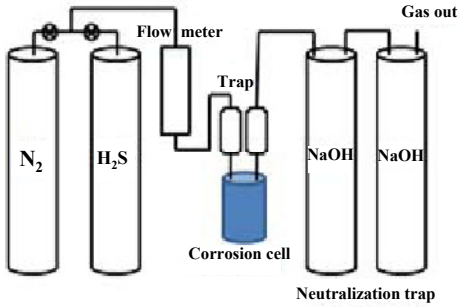

Fig. 7. Schematic diagram of the SSCC tester.

Fig. 8. The SSCC tester.

sulfide gas should be continuously supplied with a few bubbles per minute. Then, a neutralization unit should be provided for the safe treatment of the sulfide gas that flows out through the corrosion cells. Therefore, in this study, neutralization units, as shown in Fig. 7, were provided, which consisted of units that prevented the reverse flow of sulfide gas.

3.3 Test condition and procedure

The SSCC test procedure and conditions were followed on NACE TM 0177-90, and these are illustrated in Fig. 9 and Table 4. The corrosion environment was made up with a 5.0 wt.% NaCl+0.5 wt.% CH_3COOH solution. Oxygen that is dissolved in the test solution weakens the protective film that is generated by the corrosion products on the surface of the specimen and promotes the corrosion reaction. To remove the oxygen that is dissolved in the test solution, prior to the commencement of the test, the solution is purged of nitrogen gas for one hour at a rate of 100 ml/min and then saturated with hydrogen sulfide gas for 20 minutes at a rate of 100-200 ml/min. After the solution is saturated with hydrogen sulfide gas, a continuous flow of hydrogen sulfide gas is maintained at a rate of 20cc/min for the duration of the test. The maximum static stress level that is applied to the specimens is $0.9\sigma_y$ (σ_y is the yield strength of A106 Gr B steel). The SSCC resistance of specimens to the sulfide was assessed as 'failed' or 'not failed' during the duration of the test.

Table 4. Conditions of the SSCC test.

Conditions	Contents		
Static loading conditions	0.9σy, 0.8σy, 0.7σy, 0.6σy		
Conditions of the environment	Temp.	Room temperature	
	Sol.	5.0 wt.% NaCl, 0.5 wt.% glacial acetic acid, distilled water	
		pH	2.7
		Max. duration of the test	1440 hrs (2 months)
		H_2S gas saturated	20 min (100-200ml/min)
		Bubbling	A few bubbles per minute.

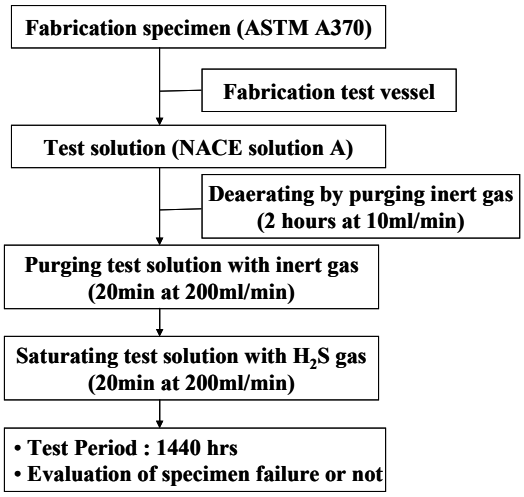

Fig. 9. The SSCC test procedure.

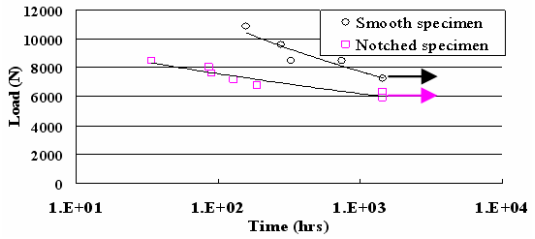

Fig. 10. Relationship between the SSCC lifetime and the load applied to multi-pass welded A106 Gr B steel in a corrosion solution that is saturated with H_2S gas.

3.4 Results of the test and discussion

Fig. 10 shows the SSCC test results for the multi-pass welded A106 Gr B steel pipe. The surfaces of the specimens were covered with the corrosion products that were generated by corrosion reaction during the test. Since the angles of failure of all failed specimens were not 45°, all specimens had failed not just by mechanical shear but by the normal SSCC mechanism. That is, when the surface pits and cracks that were generated by the SCC mechanism grew to either the critical depth or the critical size, the specimens failed. These results were also certified by fractographic observations. The failure positions of most failed specimens were at the HAZ of the weld. The reason for these results could be the complicated reaction between the welding residual stresses and the SSCC mechanism. From Fig. 10, it was evaluated that the low SSCC limit of un-notched specimens ($\sigma_{SSCCun\text{-}notched}$) was 46% (230 MPa) of the ultimate tensile strength (σ_U=502 MPa) of a multi-pass welded A106 Gr B steel pipe, while the corresponding percentage for notched specimens ($\sigma_{SSCCnotched}$) was 40% (200 MPa). Thus, $\sigma_{SSCCnotched}$ was found to be 13% lower than $\sigma_{SSCCun\text{-}notched}$

4. SCF strength assessment of a multi-pass welded A106 Gr B steel weld below the low SSCC limit

4.1 Material and specimen

The test material and configuration of the specimen for assessing the sulfide corrosion fatigue (SCF) strength and lifetime of a multi-pass welded A106 Gr B steel pipe are the same as those for the SSCC test. Since the asperity and oily particles on the surface of the specimen affect the corrosion reaction, after the surface was polished, each specimen was cleaned up by an ultrasonic washer in acetone. The sulfide corrosion fatigue (SCF) tester used a hydraulic corrosion fatigue tester (with a capacity of 20 kN). This tester was fabricated in a horizontal type to overcome the problems of the vertical type. The corrosion environments in the corrosion cell must maintain the chemical equilibrium during the test. To satisfy such conditions, the corrosion cell of Fig. 11 was fabricated with acryl and silicone bond. The rate of circulation of the test solution was controlled to be 50 ml/min.

Table 5. Conditions of the SCF test.

Conditions	Contents	
Load conditions	P_{max} (N)	7,632
	Load ratio ($R=P_{max}/P_{min}$)	0.1
Environment conditions	Temp. (°C)	Room temperature
	Corrosion solution	5.0 wt.% NaCl + 0.5 wt.% glacial acetic acid +distilled water
	pH	2.7
	Saturation	H_2S gas (≥99.5%), 20 min, 100-200 ml/min
	Bubbling	A few bubbles per minute

Fig. 11. A corrosion cell and sulfide corrosion fatigue (SCF) tester.

4.2 Test conditions and procedure

The sulfide corrosion fatigue (SCF) test conditions are illustrated in Table 5. The corrosion environments are the same as those considered in the SSCC tests. The corrosion fatigue tests were conducted for fatigue loads below the low SSCC limit(6,356 N) of the notched specimen. The load ratio (R=Pmin/Pmax) was zero and the load amplitude was constant. The applied load frequency was 0.5 Hz because the influence of the electrochemical corrosion reaction between the material and the corrosion solution is very critical in the process of corrosion fatigue failure. To maintain the chemical equilibrium due to the electrochemical corrosion reaction during the test period, the test solution was periodically changed every seven days (168 hrs) and circulated at the rate of 50 ml/min.

4.3 SCF test results

Fig. 12 shows the microstructures of the multi-pass weld: (a) the base metal; (b) the heat affected zone (HAZ); (c) the weld metal; and (d) the fracture surface that is observed after the SCF test. The specimens mostly failed at the HAZ where the high welding residual stress is distributed. As shown in Fig. 12(d), corrosion pits were generated at the boundaries of the HAZ and the base metal. This fact was verified from the assessment of electro-chemical characteristics [7]. That is, the most sensitive region in the weld in light of the sulfide corrosion environment is the HAZ, where the high welding residual stresses is distributed. Fig. 13 shows the relationship between the load range (ΔP) and the sulfide corrosion fatigue (SCF) life (N_f). The sulfide corrosion fatigue (SCF) limit, ΔP_{SCF}, was assessed under 5,081.5 (N) (equivalent stress range ($\triangle \sigma_{SCF}$) = 160 MPa) and was 32% of the tensile strength of a multi-pass welded A106 Gr B steel pipe. It was found that this ΔP_{SCF} was about 20% lower than the SSCC limit ($\sigma_{SSCCnotched}$ =200 MPa) of the notched specimen.

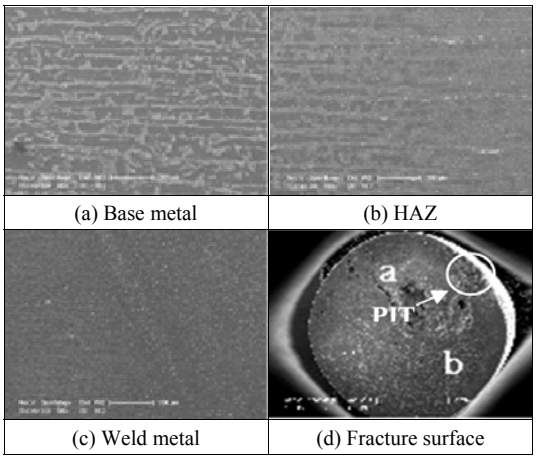

Fig. 12. Microstructure of the weld of a multi-pass welded A106 Gr B steel pipe.

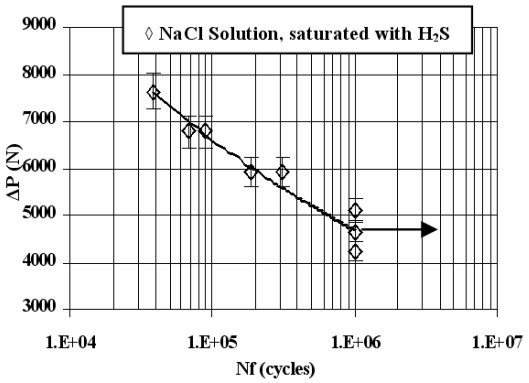

Fig. 13. The Δ P-Nf curve of A106 Gr B steel under H_2S gas solution.

5. Conclusion

After numerical and experimental analysis of the welding residual stress of a multi-pass welded A106 Gr B steel pipe, the sulfide stress corrosion cracking (SSCC) characteristics were assessed in a 3.5 wt.% NaCl solution saturated with H_2S gas at room temperature, which is in line with NACE TM 0177-90. The specimens used were of two kinds: un-notched and notched. Then, the sulfide corrosion fatigue (SCF) strength for the un-notched specimen was assessed below the low SSCC limit that earlier had been obtained from the SSCC tests for the notched specimen. From the results, the conclusions are as follows.

(1) Even though the peak stresses from FEA and the experiment were quantitatively very different from each other, the trends in the predicted residual stress distributions were very similar. The radial peak stress values from FEA were around 402 MPa; however, the experimental result yielded 160 MPa. The axial peak stress value that was predicted by FEA was 80 MPa.

(2) The low SSCC limit of un-notched specimens ($\sigma_{SSCCun\text{-}notched}$) was evaluated to be 46% (230 MPa) of the ultimate tensile strength (σ_U=502 MPa) of a multi-pass welded A106 Gr B steel pipe, while the corresponding figure for notched specimens ($\sigma_{SSCCnotched}$) was 40%(200 MPa). Thus, $\sigma_{SSCCnotched}$ was ascertained as being 13% lower than $\sigma_{SSCCun\text{-}notched}$.

(3) The sulfide corrosion fatigue (SCF) limit, ΔP_{SCF}, was assessed under 5,081.5 (N) (equivalent stress range ($\triangle \sigma_{SCF}$) = 160 MPa) and was 32% of the tensile strength of a multi-pass welded A106 Gr B steel pipe. It was found that this ΔP_{SCF} ($\triangle \sigma_{SCF}$ = 160 MPa) was about 20% lower than the SSCC limit ($\sigma_{SSCCnotched}$ =200 MPa) of the notched specimen.

References

[1] C. H. Kim, D. H. Bae, S. Y. Cho and B. K. Kim, Welding residual stress analysis and fatigue crack growth characteristics of multi-pass weld pipe

weldment, *Key Engineering Materials,* (2000) 1345-1360.
[2] D. H. Bae, S. Y. Cho, C. H. Kim, J. K. Hong and T. L. Tsai, Numerical analysis of welding residual stress using heat source models for the multi-pass weldment, *Mechanical Science and Technology* 16(9) (2002) 1054-1064.
[3] D. H. Bae and C. H. Kim, Corrosion fatigue characteristics in the weld of multi-pass welded A106 Gr B steel pipe, *Mechanical Science and Technology,* 18(1) (2004) 114-121.
[4] A. John Sedriks, B. C. Syrett, National Association of Corrosion Engineers, *NACE TM 0177-90*, (1990).
[5] D. H. Bae, S. Y. Cho, C. H. Kim, J. K. Hong and T. L. Tsai, *KSME International Journal*, 16 (9) (2002) 1054-1064.
[6] G. Y. Lee, D. H. Bae, Analysis of welding residual stress of A106 Gr B steel multi-pass welding considering the moving heat source, *KSME*, (2008) 384-389.
[7] Standard Reference Test Method for Making Potentiostatic and Potentiodynamic Anodic Polarization Measurements, *ASTM G5-94*, (2002).

Dr. Dong-Ho Bae is a professor at the school of mechanical engineering, Sungkyunkwan University in Seoul, Korea. He is currently serving as a reliability division president of the Korean Society of Mechanical Engineers. Dr. Bae's research interests are in the area of welding design, environmental strength of materials, and life prediction and reliability assessment of the industrial facilities.

Gyu-young Lee received the M.S. and Ph. D degree in mechanical engineering from Sungkyunkwan University in 2003 and 2009. Dr. Lee is currently an assistant research engineer at the KNR Systems Inc., and a member of the Korean Society of Mechanical Engineers. Lee's research interests are in the area of welding design and reliability assessment of the industrial facilities.